A&A manuscript no.
(will be inserted by hand later)

Your thesaurus codes are:
2(08.02.3; 08.06.3; 08.09.2: Aql X–1; 08.14.1)

ASTRONOMY
AND
ASTROPHYSICS
5.2.2008

The rotation speed of the companion star in Aquila X–1

T. Shahbaz[1], J. Casares[2], and P.A. Charles[1]

[1] Department of Astrophysics, Oxford University, Keble Road, Oxford, OX1 3RH, UK
[2] Instituto de Astrofísica de Canarias 38200 La Laguna. Tenerife, Spain

Received ?? ?? 1997 / Accepted ?? ?? 1997

Abstract. We have obtained medium resolution spectra of the neutron star X-ray transient Aql X–1 during quiescence. We determine the spectral type of the companion star to be K1 and also estimate its rotation speed to be $62^{+30}_{-20}\,\mathrm{km\,s^{-1}}$. By measuring the width of the Hα emission line profile of the accretion disc, we estimate the binary inclination to $\sim 50°$ and also estimate the semi-amplitude of the companion star's radial velocity curve to be $\sim$170 km s^{-1}.

Key words: binaries: general – stars: fundamental parameters, stars: individual: Aql X–1 – stars: neutron

1. Introduction

Aquila X–1(=V1333 Aquilae) is a soft X-ray transient source that shows X-ray bursts (Koyama et al. 1981; Czerny, Czerny & Grindlay 1987), thereby indicating that the compact object is a neutron star. From quiescent observationss the companion star has been identified to be a V=19.2 K-type star. The optical counterpart brightens by $\sim$2–5 magnitudes during X-ray outbursts which is interpreted as reprocessing of radiation in the accretion disk (Thorstensen, Charles & Bowyer 1978, hereafter TCB; Canizares, McClintock & Grindlay 1979; Charles et al. 1980; van Paradijs et al. 1980).

Attempts to find the orbital period have revealed many variations but no firm period. Watson (1976) reported an unconfirmed 1.3 day X-ray periodicity during the 1975 outburst. Chevalier & Ilovaisky (1991) have obtained an 18.97 hr periodicity from optical photometry during its active state, which they interpret as being the orbital period.

TCB observed the optical counterpart in its low state. They found the only significant feature in the spectrum was the Mg*b* 5175Å blend in absorption; no Balmer lines were evident. They concluded that the spectrum is characteristic of a K0-3 V star. Shahbaz et al. (1996) also obtained low resolution spectra of Aql X–1 in quiescence. They too found the Mg*b* absorption blend but also Hα and the Paschen series in emission. They found by fitting the continuum spectrum that it could be best described by a K5 star.

Aql X–1 is known to undergo regular X-ray and optical ourbursts on a timescale of $\sim$1 year (Kaluzienski et al. 1977; Priedhorsky & Terrell 1984; Charles et al. 1980) much more frequently than the other neutron star transient Cen X–4 (McClintock & Remillard 1990). Recently the RXTE All Sky Monitor showed Aql X–1 to be have undergone an X-ray outburst between late January and early March 1997 (Levine & Thomas 1997). Ilovaisky & Chevalier (1997) reported that Aql X–1 was optically in quiescence by 30 March 1997. In this letter we report on our medium resolution spectra of Aql X–1 obtained in May 1997, when the source was in quiescence. We were able to determine the spectral type of the companion star and also its rotation speed.

2. Observations and data reduction

We obtained intermediate resolution spectra of Aql X–1 on 13 May 1997 using the 3.9-m Anglo-Australian Telescope at Siding Spring, Australia. A Tek 1024^2 CCD attached to the RGO spectrograph was used during all the observations. The 600V grating was centered at 5190Å giving a dispersion of 1.55 Å pixel^{-1} and a spectral resolution of 3.6Å (FWHM=165 km s^{-1} at Hα). We took 10 spectra of Aql X–1 each with an exposure time of 1800 secs starting at 14:58 UT with interspaced Cu-Ar arc spectra for wavelength calibration. Template field stars of a variety of spectral types were also observed.

The data reduction and analysis was performed using the Starlink FIGARO package, the PAMELA routines of K. Horne and the MOLLY package of T. R. Marsh. Removal of the individual bias signal was achieved through subtraction of the mean overscan level on each frame. This was acceptable since an examination of the bias frames

Send offprint requests to: T. Shahbaz (tsh@astro.ox.ac.uk)

showed no significant structure. Small scale pixel-to-pixel sensitivity variations were removed by multiplying by a flat-field frame prepared from observations of a tungsten lamp. One-dimensional spectra were extracted using the optimal algorithm of Horne (1986), and calibration of the wavelength scale was achieved using 4th order polynomial fits giving an rms scatter of 1/12th of a pixel (0.13Å).

Table 1. Optimal Subtraction of the Companion Star

Star	Sp. Type	χ^2 (DOF=907)	vsin i	f
HR 805	G8III	794.2	64	1.05±0.03
HR 794	K0III	779.5	62	1.09±0.04
HR 807	K1III	776.6	62	0.94±0.03
HR 822	K2III	927.2	66	0.77±0.03
HR 872	K3III	900.6	66	0.60±0.02
HR 871	K4III	1040.4	36	0.55±0.02
HR 851	K5III	861.6	50	0.70±0.02

3. The spectral type and rotational broadening of the companion star

We determine the spectral type of the companion star by minimizing the residuals after subtracting different template star spectra from the Doppler-corrected average spectrum. This method is sensitive to the rotational broadening $v \sin i$ and the fractional contribution of the companion star to the total flux (f; 1-f is the "veiling factor").

First we determined the velocity shift of the individual spectra of Aql X–1 with respect to each template star spectrum by the method of cross-correlation (Tonry & Davis 1979). The Aql X–1 spectra were then interpolated onto a logarithmic wavelength scale (pixel size 80 $\mathrm{km\,s^{-1}}$) using a sin x/x interpolation scheme to minimize data smoothing (Stover et al. 1980). No significant velocity variations were observed (see section 4), so we averaged the Aql X–1 spectra to the rest frame of the template star.

In order to determine the rotational broadening $v \sin i$ we follow the procedure described by Marsh, Robinson & Wood (1994). Basically we subtracted a constant representing the fraction of light from the template star, multiplied by a rotationally broadened version of that template star. We broadened the template star spectrum from 0 to 200 km $\mathrm{s^{-1}}$ in steps of 1 km $\mathrm{s^{-1}}$ using the Gray rotation profile (Gray 1976). We then performed an optimal subtraction between the broadened template and averaged Aql X–1 spectra. The optimal subtraction routine adjusts the constant to minimize the residual scatter between the spectra. The scatter is measured by carrying out the subtraction and then computing the χ^2 between this and a smoothed version of itself. The constant, f, represents the fraction of light arising from the template spectrum, i.e. the secondary star. The optimal values of $v \sin i$ and f are obtained by minimising χ^2 (see Table 1). The above analysis was performed in the spectral range 5120–6710 Å excluding the Hα emission line and the interstellar feature at 5190 Å. A linear limb-darkening coefficient of 0.76 was used (Al-Naimiy 1978) appropriate for 6000 Å and an effective temperature of 4500 K (typical for a K star). We also performed the above analysis using zero and full limb-darkening and only obtained a change in $v \sin i$ of at most 4 $\mathrm{km\,s^{-1}}$.

From Table 1 it can be seen that the minimum χ^2 occurs at spectral type K1 with a $v \sin i$ of 62^{+30}_{-20} $\mathrm{km\,s^{-1}}$(1-σ) and the companion star contributing about 94% to the observed flux at $\sim$ 6000 Å. Fig. 1 shows the results of the optimal subtraction and the $\chi^2 - v \sin i$ plot is shown in Fig. 2. All the template stars used in the above analysis were of luminosity class III. The effects of using different luminosity class spectra in the analysis was estimated by comparing the absorption line flux density of stars of different spectral type and class. We find using template stars of spectral type K1, K4 and K7 and luminosity class V and III, the flux density of the stars of different luminosity class (but the same spectral type) are only different at the 1 percent level. Therefore, the value we obtain for f in the above analysis is not dependant on the luminosity class of the template star used.

In order to verify the validity of the minimum in the $\chi^2 - v \sin i$ plots we performed the same analysis on a template star. The broadening in the template star spectrum is dominated by the instrumental broadening. To this template star we added noise to produce a spectrum of comparable quality to our Aql X–1 data. The above broadening and optimal subtraction procedure was then repeated, The results are shown in Fig. 2, where the minimum χ^2 occurs when no broadening is used. This is exactly as expected since the template star spectrum must be dominated by instrumental broadening. Therefore we are confident that the minimum χ^2 for the Aql X–1 spectrum is real, although the errors in the $v \sin i$ determination are large.

4. The Aql X–1 spectrum

In Fig. 1 we show the variance-weighted average of the Aql X–1 spectra, which has a signal-to-noise ratio of about 25 in the continuum. The most noticeable feature is double peaked Hα emission which has a broad base (FWZI$\sim$2000 $\mathrm{km\,s^{-1}}$). We tried to see if there was any velocity variation in the absorption lines by cross-correlating the individual Aql X–1 spectra with a template star (HR 807), but found no significant variation over the 5 hr baseline. Therefore we quote the mean heliocentric systemic velocity obtained from the averaged Aql X–1 spectrum of 57±21 $\mathrm{km\,s^{-1}}$(the template star used, HR 807, had a heliocentric velocity of 15±16 $\mathrm{km\,s^{-1}}$). Again from the averaged Aql X–1 spectrum the equivalent width

Fig. 1. The results of the optimal subtraction. From top to bottom: the variance-weighted average spectrum of Aql X–1, the template K1III star (HR 907) broadened by 62 km s^{-1}, the residual spectrum of Aql X–1 after subtracting the template star times f=0.94. The spectra have been normalized and shifted vertically for clarity. The right inset shows a close-up of the smoothed double-peaked Hα emission line profile in the Aql-X–1 spectrum. The left inset shows a close-up of the Hα residual spectrum with FWHM=816$\pm$40 km s^{-1}.

of Hα is 5.3$\pm$0.3Å with a mean heliocentric velocity of 99$\pm$30 km s^{-1}, obtained using a single Gaussian fit.

5. Discussion

5.1. The binary inclination

After subtracting the spectrum of the companion star from the Aql X–1 spectrum, the most noticable feature is the single peaked Hα emission line (presumably arising from the accretion disc) with a FWHM velocity of 816$\pm$40 km s^{-1}(see Fig. 1). This is in contrast to the observed Aql X–1 spectrum which shows a double-peaked profile, implying that the core of the double-peaked profile is due to the Hα absorption line arising from the secondary star.

We can compare the accretion disc Hα emission line in Aql X–1 with that in Cen X–4 since both have neutron star primaries and probably similar orbital periods. The width of the disc Hα emission line in Cen X–4 is 687$\pm$20 km s^{-1}(FWHM; Casares et al. 1997) whereas it is broader in Aql X–1, which suggests that the binary inclination of Aql X–1 may be higher than that of Cen X–4. If we assume Keplerian motion in the accretion disc and that the mass of the compact object, and orbital period of the two systems are comparable, then the velocities in the disc simply scale with sin i (Frank, King & Raine 1992). Using the velocity widths given above for Aql X–1 and Cen X–4 and the binary inclination for Cen X–4 (40°; Shahbaz, Naylor & Charles 1993), we estimate $i \sim 50°$ for Aql X–1.

It should however, be noted that the assumption of Keplerian velocities at the outer edge of the disc may not hold (Orosz et al. 1994). For a system at such an inclination one might have expected to see a double-peaked emission line profile, arising from an accretion disk viewed at high inclination. However, there are probably other sources of Hα emission from the system which contaminate the disc profile, such as from the heated face of the secondary star or from the bright spot. Also note the poor resolution and signal-to-noise of our data, therefore we cannot rule out a high binary inclination on the lack of a double-peaked profile alone.

5.2. The K_2 velocity

If the orbital period is 18.97 hr and the secondary star fills its Roche lobe, then the density of the secondary star is ρ=0.3 g cm^{-3}. A K1 main sequence star would have ρ=1.9 g cm^{-3}., implying that the radius of the secondary star must be about twice that of a main sequence star in order for it to fill its Roche lobe. It is therefore likely to be evolved, similar to the secondary star in Cen X–4 (Shahbaz, Naylor & Charles 1993). If we believe the estimate to the binary inclination to be $\sim 50°$, and that both systems have similar mass compact objects, then one can estimate K_2 for Aql X-1 (K_2 scales with sin i c.f. the mass function equation). Using K_2=146 km s^{-1}(McClintock & Remillard 1990) and $i = 40°$ for Cen X–4 and $i = 50°$ for Aql X–1 we estimate K_2 for Aql X–1 to be $\sim$170 km s^{-1}.

Fig. 2. The $\chi^2 - v \sin\, i$ analysis plot for Aql X–1 (shown as the histogram) using the template star HR 907. The minimum χ^2 (χ^2_{min}) is found with a rotational broadening of 62 km s^{-1}. The 68% confidence level (χ^2_{min}+1) is also marked as the dashed horizontal line. Also shown is the result for simulated data using a template star shown as the solid line. Note that χ^2_{min} occurs at zero broadening, which implies that the minimum in the Aql X–1 $\chi^2 - v \sin\, i$ plot is real. The right abscissa refers to the template star χ^2 values.

6. Conclusions

Using medium resolution optical spectra, we have determined the spectral type of the companion star in the neutron star X-ray transient system Aql X–1, to be a K1 star. By optimally subtracting different broadened versions of the companion star spectrum from the average Aql X–1 spectrum we determine the rotational broadening of the companion star to be 62^{+30}_{-20} km s^{-1}, with a contamination of $\sim$ 6% to the observed flux at 6000Å. We also estimate the binary inclination to be $\sim 50°$ by measuring the width of the accretion disc Hα emission line, and K_2 to be $\sim$ 170 km s^{-1}.

Acknowledgments

We are grateful to all the staff at the AAT, Siding Spring in particular our telescope operator Jonathan Pogson. The data reduction was carried out on the Oxford Starlink node, and the figures were plotted using the ARK software.

References

Canizares, C.R., McClintock, J.E., Grindlay, J.E., 1979, 236, L55
Charles, P.A., et al. 1980, ApJ, 249, 567
Chevalier, C., Ilovasiky, S.A., 1991, A&A, 251, L11
Czerny, M., Czerny, B., Grindlay, J.E., 1987, ApJ, 312, 122
Frank, J., King, A.R., Raine, D.J., 1992, Accretion Power in Astrophysics, Cambridge University Press, Cambridge, p54
Gray, D.F., 1976, The Observations and Analysis of Stellar Photospheres, Willey-Interscience, New York
Horne, K., 1986, PASP, 98, 609
Horne, K., Marsh, T.R., 1986, MNRAS, 218. 761
Kaluzienski, L.J., et al., 1977, Nat, 265, 606
Ilovasiky, S.A., Chevalier, C., 1997 IAU Circ. 6638
Levine, A.M., Thomas, B., 1997, IAU Circ. 6558
Koyama, K.,1981, ApJ, 247, L27
McClintock, J.E., Remillard, R.A., 1990, ApJ, 350, 386
Marsh, T.R. Robinson, E.L., Wood, J.H. 1994, MNRAS, 266, 137
Orosz, J.A., Bailyn, C.D., Remillard, R.A., McClintock, J.E., Foltz, C.B., 1994, ApJ, 436, 848
Paczynski, B., 1971, ARA&A, 9, 183
Priedhorsky, W.C., Terrell, J., 1980, ApJ, 280, 661
Shahbaz, T., Naylor, T., Charles, P.A., 1993, MNRAS, 265, 655
Shahbaz, T., Smale, A.P., Naylor, T., Charles, P.A., van Paradijs, J., Hassall, B.J.M., Callanan, P., 1996, MNRAS, 282, 1437
Stover, R.L., Robinson, E.L., Nather, R.E., Montemayer, T.J., 1980, ApJ, 240, 597
Thorstensen, J., Charles, P.A., Bowyer, S., 1978, ApJ, 220, L131
Tonry, J., Davis, M., 1979, AJ, 84, 1511
van Paradijs, J., Verbunt, F., van der Linden, T., Pederson, H., Wamsteker, W., 1980, ApJ, 241, L161
Watson, M.G., 1976, MNRAS, 176, 19

This article was processed by the author using Springer-Verlag LaTeX A&A style file *L-AA* version 3.

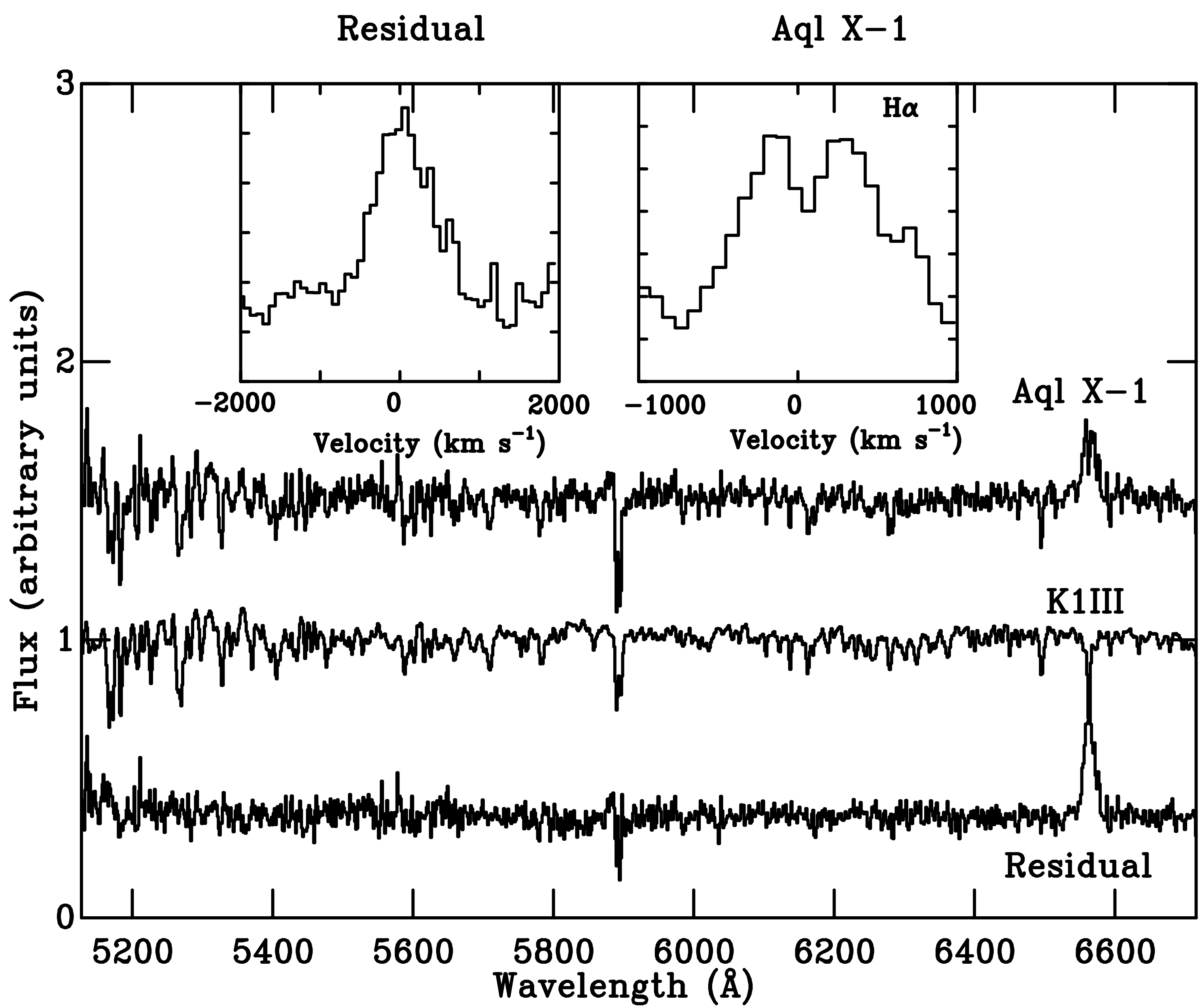

Residual
Aql X−1
Hα
−2000
0
2000
Velocity (km s^{-1})
−1000
0
1000
Velocity (km s^{-1})
Aql X−1
K1III
Residual
Flux (arbitrary units)
0
1
2
3
5200
5400
5600
5800
6000
6200
6400
6600
Wavelength (Å)

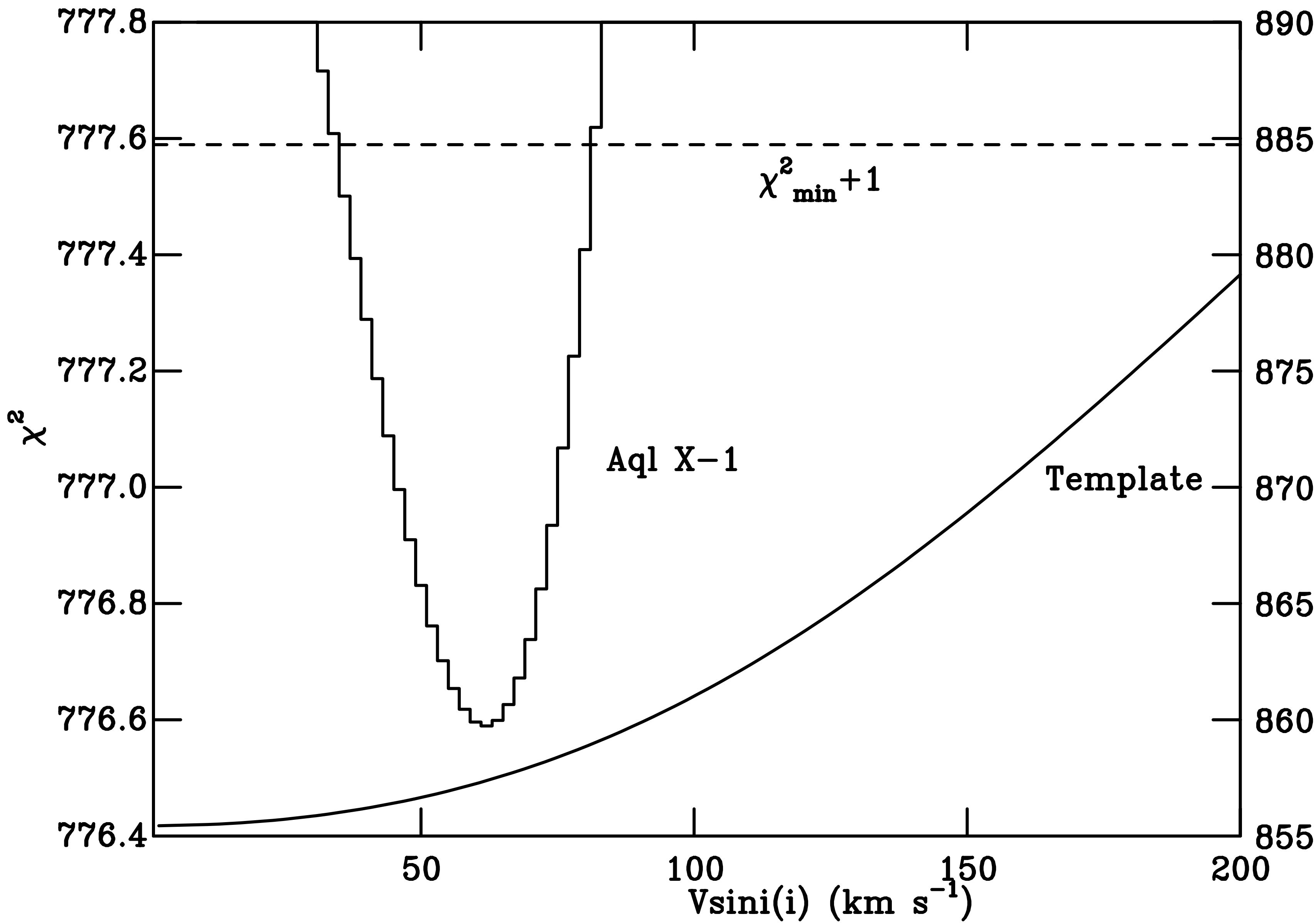
777.8
777.6
777.4
777.2
777.0
776.8
776.6
776.4
χ^2
890
885
880
875
870
865
860
855
50
100
150
200
Vsini(i) (km s^{-1})
χ^2_{min}+1
Aql X−1
Template